Taylor & Francis
Taylor & Francis Group

Journal of Maps

ISSN: 1744-5647 (Online) Journal homepage: www.tandfonline.com/journals/tjom20

Stratigraphy and volcano-structural evolution of the Montiferru Volcanic Complex, Sardinia

Costantino Pala, Stefano Naitza & Laura Pioli

To cite this article: Costantino Pala, Stefano Naitza & Laura Pioli (2026) Stratigraphy and volcano-structural evolution of the Montiferru Volcanic Complex, Sardinia, Journal of Maps, 22:1, 2632982, DOI: 10.1080/17445647.2026.2632982

To link to this article: https://doi.org/10.1080/17445647.2026.2632982

JOURNAL OF MAPS
2026, VOL. 22, NO. 1, 2632982
https://doi.org/10.1080/17445647.2026.2632982

Stratigraphy and volcano-structural evolution of the Montiferru Volcanic Complex, Sardinia

Costantino Pala[a], Stefano Naitza[a,b] and Laura Pioli[a]

[a]Dipartimento di Scienze Chimiche e Geologiche, Università degli Studi di Cagliari, Monserrato, Italy; [b]CNR-IGAG, Cagliari, Italy

ABSTRACT

The Montiferru Volcanic Complex in Sardinia (Italy) records a complex interplay of volcanic cycles and sedimentation but lacks a comprehensive geological framework. Here we present a new 1:50.000 scale volcano-structural map defining twelve unconformity-bounded stratigraphic units that delineate Miocene to Pleistocene volcanic and sedimentary phases, including caldera-forming eruptions, dome field formation, flank collapses, and monogenetic activity. Integrated field mapping, petrography, and geochronology revealed the occurrence of distinct volcanic centers and a defined structural evolution of the complex. Notably, we identify Miocene and Pliocene hydrothermal mineralization phases characterized by siliceous sinter and anomalous Au, Ag, As, and Hg concentrations, linked to multiple epithermal systems within varied volcanic settings. These findings refine the eruptive history and provide a structural basis for mineralization processes in the Montiferru Complex.

ARTICLE HISTORY
Received 24 September 2025
Revised 6 December 2025
Accepted 8 December 2025

KEYWORDS
Volcanic stratigraphy; low-sulfidation; unconformity bounded stratigraphic units; ore deposit exploration; volcanic complex; geological map

1. Introduction

The Montiferru Volcanic Complex (40°08′52.67″N, 8°36′14.51″E) is located in west Sardinia (Figure 1, Figure S3), is 1.200 km^2 wide developed within two distinct regional volcanic cycles (Di Battistini et al. 1990; Fedele et al. 2007). The oldest cycle, of Oligocene–Middle Miocene age, is associated with arc volcanism and back arc extension due to the Apennines–Maghrebides subduction, which was associated to predominantly explosive activity and emission of calc-alkaline andesite to rhyolite magmas, with an eruptive peak during Aquitanian–Burdigalian (Carminati et al. 2012). The most recent cycle, of Pliocene–Pleistocene age, emitted lavas with composition ranging from alkaline basanite to tephrite and phonolite, within an extensional setting due to slab roll back and westward migration of the back arc region and formation of the Tyrrhenian basin (Carminati et al. 2012). Between the two magmatic cycles, during the Middle–Upper Miocene, several small basins formed on the west of the island, determining a marine transgression and deposition of shallow-water limestones and marl deposits (Faccenna et al. 2002). The complex developed over a Variscan basement (Figure 1; Carmignani et al. 2008).

Previous mapping of the area at the 1:50.000 and 1:100.000 scales (Assorgia et al. 1981; Dannemberg 1905; Deriu et al. 1988) mainly focused on the petrographic characteristics of the rock units, underlying their compositional variability, which ranged from calcalkaline andesite to rhyolites (Miocene cycle) to alkaline basanite to tephrite and phonolite lavas (Plio-Pleistocene cycle).

Only a few studies focused on the Plio-Pleistocene volcanic activity included both chemical composition and geochronological data (Beccaluva et al. 1977, 1983; Coulon et al. 1974; Fedele et al. 2007; Fibbi 1970; Savelli et al. 1979; Zerbi et al. 1978); the most recent work published on the petrology and evolution of the edifice distinguished four volcanic phases, starting with the emplacement of analcime-basanite lava flows, followed by trachyte to phonolite lava domes and flows generated by magmas fractionation in small chambers and interaction with crustal lithologies. A third phase is marked by the emission of basalt lava flows, and a later phase of analcime basanite lava flows fed by new magma batches with minor and no substantial differentiation Fedele et al. (2007).

Small volume ore mineral deposits (Fe oxides and sulfides; Cu-Pb-Zn sulfides; Pb carbonate) are known in all the western sector of Montiferru and described for the first time by La Marmora (1857). Iron ore was mined since early historic times and until Second World War (Moscati et al. 1997; Ministero dell'Industria e del Commercio 1940). The ore were later investigated by Fadda (1993), Fadda et al.

CONTACT Costantino Pala costantino.pala@unica.it Dipartimento di Scienze Chimiche e Geologiche, Università degli Studi di Cagliari, Cittadella Universitaria di Monserrato, Blocco A, 09042 Monserrato, CA, Italy
Supplemental map for this article can be accessed online at https://doi.org/10.1080/17445647.2026.2632982

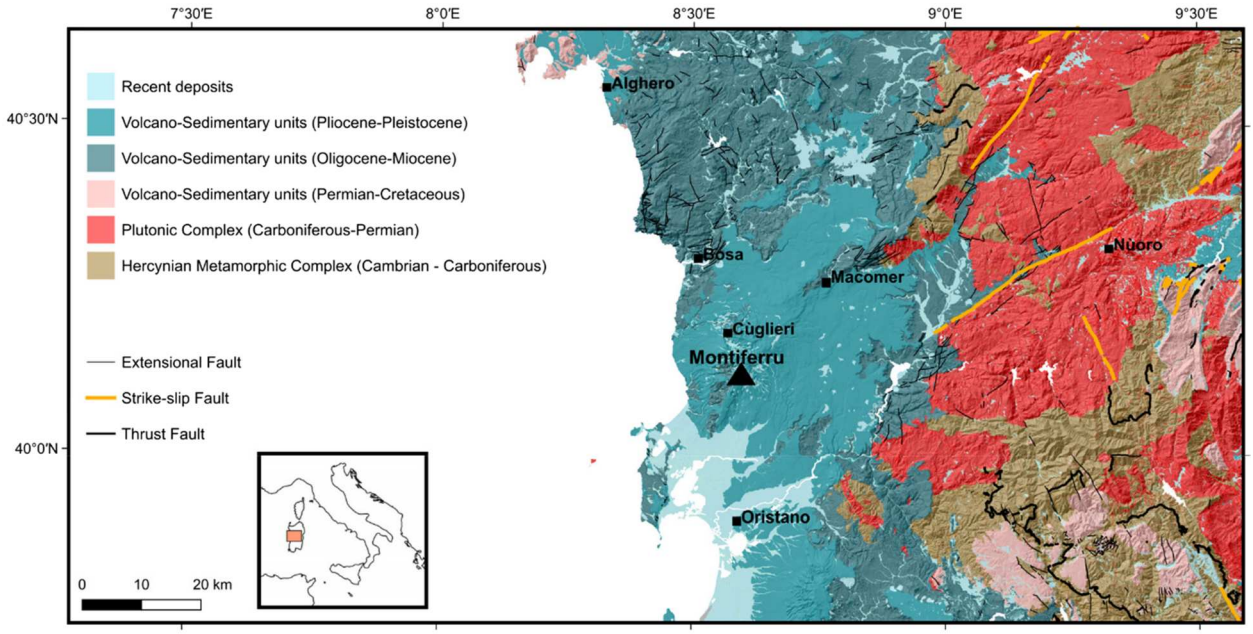

Figure 1. Regional geological map with Montiferru in the frame of the Sardinian Magmatic Province in central Sardinia. Geology and structural data are from https://www.sardegnageoportale.it Mute map modified from https://www.freeworldmaps.net.

(1998), Grillo et al. (1993) and became targets for mineral exploration when the whole region emerged as highly prospective for precious metals (Boi et al. (1997); Gold Mines of Sardinia LTD 2000). In the southern part of this area, mineralization is hosted in Miocene andesite domes and PDC deposits. The ore consists of iron rich quartz veins mainly containing hematite and chalcopyrite with minor sphalerite, galena, tetrahedrite and up 5.7 ppm gold (Fadda 1993). In the northern sector, the ore is hosted in Pyroclastic Density Current (PDC) deposits, and hot spring deposits occur near the Cùglieri, Scano Montiferro and Tresnuraghes towns (Fadda 1993; Gold Mines of Sardinia LTD 2000; La Marmora 1857). However, the mineralizing stages were not clearly defined, and the role of the most recent volcanic phase in fostering hydrothermal systems mineral deposition was, before the beginning of this study, unknown. Ore bodies generated by hydrothermal systems associated with alkalic magmatism are among the richest in Au Kelley et al. (2020) but they are also relevant for the potential occurrence of F, Platinum Group Elements (PGE), Rare Earth Elements (REE), Te, Ti, V, and W (Bissig and Cooke 2014; Kelley et al. 2020; Kelley and Spry 2016; Pirajno 2009). Hydrothermal systems fed by calc-alkalic and alkalic magma suites typically results in different fluid compositions and so, in distinct ore bodies (Simmons et al. 2005). Multiple hydrothermal phases result into a complex mineralization in the same area. Mineral exploration in these complex ore systems requires a clear structural model, identification of the number and types of superimposed epithermal systems, their classification and, consequently, definition of the spatial distribution of the potential target elements. In this work, we are presenting a new map of the Montiferru area at the scale 1:50.000 to share a comprehensive volcano structural framework providing all the key information on the formation and evolution of the volcanic activities and the fundamental dataset for the interpretation of the hydrothermal systems which formed the mineral deposits.

2. Materials and methods

2.1. Mapping

The initial activity consisted in a critical and systematic revision of the previously published geological map of the area (Assorgia et al. 1981; Deriu et al. 1988) followed by preliminary field surveys. Major geological lineations and lithosome boundaries were identified through landform analysis using a 10 m resolution Digital Elevation Model (DEM) and aerial photography. Field surveys were conducted from 2019 to 2022 to check the validity of the mapped units and identify and interpret the main volcanic structures of the area. Regional unconformities were defined according to the geological map of Sardinia at 1:250.000 scale (Carmignani et al. 2008). Lithosomes were grouped into Unconformity Bounded Stratigraphic Units (UBSU) such as Synthems and Subsynthems (Salvador 1987; Table 1). Minor unconformities, extending only in limited portions of the studied area, were considered for the identification of informal units, which grouped adjacent lithosomes and marked main variations in the style of volcanic activity or distinct sedimentary events.

Table 1. Description of the synthems proposed in this work.

Epoch	Synthem	Subsynthem	Informal unit	Description	Age (Ma)
Early-Middle Miocene	Sirìsi [A]		Sa Montrarba [Aam]	Volcanic breccia and Lava flows and dikes	
			Aúrras [Aau]	Welded PDC deposits	
	Disconformity/Erosion of Aam and Aau. Erosion of Aam and Aau. Absence of hydrothermal alteration. At least 200 metres of erosion before Porto Alabe deposition (Fadda, 1993).				
	Porto Alabe [Ab]		–	Fallout, Lava domes and PDC deposits	18.0±0.7[a]
Middle Miocene	Nonconformity/Regional subsidence Allevi et al. (2025). Cessation of volcanic activity				
Middle–Late Miocene	Santa Caterina [B]	–	–	Limestones in littoral facies, and subordinate fluvial sandstones	–
Late Miocene–Early Pliocene	Nonconformity/Regional Uplift Allevi et al. (2025). New volcanic activity, different eruptive style.				
Pliocene	Ghísos [C]	Sa Tànca Nòa [Ca]	Pèdra Onàda [Cap]	Aa lava flows intercalated with alluvial fan deposits	3.9±0.3[b] 3.86±0.05[c]
			Tuvonari [Cat]	Lava flows and domes, minor pyroclastic deposits	3.65±0.03[b] 3.2±0.2[d]
		Disconformity: Volcano flank collapse			
		Cùglieri [Cb]	Canighèrbu [Cbc]	Volcanic Debris avalanche	–
			Bàdu de Papéri [Cbb]	Deposits, debris flow deposits, Alluvial fan deposits	–
			Fàche de Sòle [Cbf]		–
		Buttress unconformity or Disconformity Contact on the scar collapse Disconformity Contact on the Cùglieri subsynthem and older units			
		Mùrcuneddu [Cc]	–	Lava flows, domes and dikes	2.8±0.1[e]
Upper Pliocene–Pleistocene	Angular unconformity/Erosion (Assorgia et al., 1981; Deriu et al., 1988). Local paleosols				
	Campèda [D]	Bonarcado [Da]	–	Paheohe to aa lava flows, dikes. Alluvial fan deposits.	3.14±0.08[c] 3.10±0.2[f] 3.01±0.09[f] 3.0±0.2[d] 2.9±0.2[d] 2.8±0.1[e] 2.7±0.2[d] 2.5±0.1[f]
		Angular unconformity Paleosols, erosion, change in the eruptive style			
		Sèneghe [Db]	–	Scattered monogenetic cones associated with lava flows.	2.3±0.2[d] 1.57±n.a.[g]
Upper Pleistocene–Holocene	Nonconformity/End of volcanism, formation of soils, erosion				
	Portovesme [E]	Portoscuso [Ea]	–	Aeolian Sands	–

Radiometric ages from a: Savelli et al. (1979), b: Fibbi (1970); c: Fedele et al. (2007); d: Beccaluva et al. (1977); e: (Coulon et al., 1974); f: Beccaluva et al. (1983); g: Zerbi et al. (1978).

In parallel, we made a critical review of the published data and a field study of ore bodies and hydrothermal alterations. Data were compared with new analytical data on mineral assemblages on altered units to further compile a hydrothermal facies map.

2.2. Mineralogical analyses

X-ray diffraction (XRD) analyses were performed on nineteen selected specimens of altered rocks (Table S1) using the Panalytical Empyrean diffractometer located in the Department of Chemical and Geological sciences of the University of Cagliari. Analyses were performed using laboratory θ–2θ equipment and operating at 40 kV and 40 mA with Cu Kα radiation (λ = 1.54060 Å) and using the X'Celerator detector.

2.3. Petrology and geochronology

A dataset of all available published material on the composition and petrographic properties of the unit was compiled based on published sources. A geochronologic dataset was compiled based on published material (Table 1). Basic petrographic investigation on thin sections from selected specimens was made to confirm previously published data on mineral content of volcanic rocks.

2.4. Map production

Geological map and analysis produced using QGIS (v. 3.34) and Inkscape (v. 1.4). The layout includes:

(a). Main map with geological units, structural symbols, and infrastructure overlaid on a 2x hillshade base (Figure S1 in the map);
(b). Hydrothermal alteration map showing alteration patterns over gray-toned volcanic cycles, including a location inset (Figure S4 in the map);
(c). Chronostratigraphic scheme at the synthem scale (Figure S2 in the map);
(d). Geological cross-sections generated via the qgSurf Plug-in (v. 3.2.2) and Inkscape v1.4 with subsynthem color coding (Figures S5 and S6 in the map). The **main map** features a topographical base (2x hillshade) overlaid with unconformity bounded stratigraphic units (UBSU), contour lines, structural symbols, the hydrographic and road networks, major toponyms, radiometric age symbols, and unit labels.

The **hydrothermal alteration map** uses a limited topographical base (2x hillshade) where UBSU are categorized by volcanic cycle in gray tones, while colored areas define the alteration limits. This section also includes a location inset map within the European context (Figure S3 in the map). The **chronostratigraphic scheme** was designed in Inkscape at the subsynthem scale, with each subsynthem color-coded to the map. Finally, **geological cross-sections** were generated using the QGIS qgSurf Plug-in (v. 3.2.2) and Inkscape v1.4, employing a 2x topography overlaid with sub-synthem color coding. Inkscape was used to complete the profiles.

3. Results

We grouped stratigraphic units into eleven unconformity bounded stratigraphic units (Table 1, Figure S2):

3.1. Miocene

3.1.1. Sirìsi synthem (Aquitanian–Burdigalian?)

The Sirìsi synthem is the oldest unit (Figure S2) and is composed by volcanic products of an eruptive center located in the SW of the study area. The synthem is exposed mainly in the western sector of the Complex, and its thickness locally exceeds 400 m. It is subdivided into two informal units: Aúrras and Sa Montrarba, separated by a high-angle unconformity, which we interpret as a caldera ring fault (Figures S1 and S6 in the map). Sa Montrarba comprises the inner caldera deposits such as hydrothermally altered pyroclastic breccia cut by lava (dykes and shallow intrusions) and quartz veins. Breccia deposits contains scattered clasts of granitoids (Figure 2a). Aúrras comprises the deposits outside the caldera and consists of a succession of welded PDC deposits separated by paleosols and/or fallout pumice layers, and epiclastic deposits (Figure 2b). The ignimbrites are typically porphyritic for mm-sized crystals of sanidine, plagioclase, pyroxene and biotite and display rhyolite to dacite compositions. On the other hand, Sa Montrarba deposits shows pervasive alteration and include hydrothermal ore deposits. Ore deposits formed at depths of 200 m or higher (Fadda, 1993). No geochronological data are available for this synthem.

3.1.2. Porto Alabe synthem (Burdigalian)

This unit is lying in disconformity over Sirìsi synthem (Figure S1, S5 in the map). The disconformity is associated with an erosional surface and a diffuse paleosoil (Figure S4 in the map). The Porto Alabe synthem consists of lava domes, variably welded PDC deposits (Figure 2c), ash to small lapilli pumice fallout and epiclastic layers of variable composition and crystal content. The uppermost deposit is a non-welded ignimbrite, containing porphyritic pumice comprising crystals of quartz, plagioclase, clinopyroxene, and sanidine, biotite. Lithic clasts consist of welded ignimbrite and aphyric lava fragments. The ignimbrite shows no significant variability in the studied area, suggesting that it is part of a very large unit formed in a large magnitude, possibly caldera forming eruption sourced outside the study area. Only one dating (18.0 ± 0.7 Ma K/Ar) from this synthem is available in the literature and corresponds to the uppermost rhyolitic ignimbrite (Savelli et al., 1979; Figure S1).

Figure 2. Photos for the Miocene units. Sirìsi synthem: Polymict caldera collapse breccia of the Sa Montrarba Unit (a); Ignimbrites of the Aúrras Unit (b) Reomorphic ignimbrite of the Porto Alabe Volcano (c). Santa Caterina Synthem: Marls and limestones (d).

3.1.3. Santa Caterina synthem (middle–late Miocene)

This synthem consists in a succession of marls, limestones, and terrigenous sandstones formed from Middle to Upper Miocene (Figure S2 in the map) associated with end of volcanism, the formation a series of small basins associated with backarc extension and rotation of the Sardinia–Corsica block (Faccenna et al., 2002). The nonconformity is an erosional surface covered by marine to littoral sedimentation. The maximum exposed thickness of the succession is of 50 m (Figure S1 in the map). Layers are locally tilted up to 32° in areas adjacent to the lava dome field of the Ghísos synthem to sub-horizontal in the other areas. The basal layer is exposed in the northern sector, where the deposits lie over Porto Alabe. It consists of a volcanoclastic breccia embedded in carbonatic matrix with sparse fossil content. Marls are ivory-coloured (Figure 2d), locally reworked by syndepositional slumping into breccia bodies. They have a relatively scarce fossil content limited to Pecten sp. and fragments of echinoids (Mancosu et al. 2022). Limestones are white to ivory and consist of coralline algal grainstones to rudstones (Mancosu et al. 2022). The succession is formed in an outer sublittoral environment, at moderate sea depth (Mancosu et al. 2022). In the northern exposures close to Scano di Montiferro the unit consists in fluvial sandstones. Their structures, consisting of ripple, cross laminated sand, or cross bedded layers containing very fine sand to very coarse sand suggest lower flow regime in river channel, bar, and overbank facies (Sr facies, Miall 2006).

Miocene units are cut by normal faults sealed by the Plio Pleistocene units (Figure S1 in the map). These are probably associated with the regional uplift associated with migration of the back arc extension to the W of the island (Carminati et al. 2012).

3.2. Plio-Pleistocene

3.2.1. Ghísos synthem (Zanclean–Piacenzian)

The Ghísos synthem groups the lithosomes associated with a renewed volcanic activity following a regional uplift and emersion of the area testified by a nonconformity (Figures S1, S2, S5, S6 in the map). The unconformity is represented by a erosional surface followed by alluvial fans, revealing the general uplift and resume of continental erosion in the area. It consists of dome-lava flow fields interbedded with alluvial fans, debris avalanche, and debris flow deposits. Three subsynthems, respectively associated with a major phase of edifice construction, a multiple collapse phase, and a final eruptive phase, were identified:

– Sa Tànca Nòa subsynthem
– Cùglieri subsynthem
– Mùrcuneddu subsynthem

3.2.1.1. Sa Tànca Nòa subsynthem (Zanclean–Piacenzian). The Sa Tànca Nòa subsynthem consists of a succession of sedimentary deposits, lava flows and domes and interbedded alluvial fan deposit lying in unconformity over both lower synthems and reaches a thickness of up to 300 m. It was divided into two informal units, Pèdra Onàda and Tuvonari, which marks a shift in volcanic activity and vent location.

Pèdra Onàda unit consists of alluvial fans of massive breccia made of cobbles, pebbles, and blocks, dispersed in a sandy-clay matrix. Basanite to tephrite lava flows 1–3 m thick are interbedded in the breccia deposit (Figure 3a). Breccia mainly consists of Sirìsi volcanics (welded ignimbrites altered volcanics) in the lower layers, accompanied by basanite lava blocks in the upper layers.

Lava flows are either isolated or intercalated with the alluvial deposits, are typically porphyritic for euhedral to subhedral pyroxene, amphibole and phlogopite crystals, ranging in size from few millimeters to 5 cm. Cm-sized granulite (Montanini & Harlov 2006) and rare mantle xenoliths are embedded in the lava (Fedele et al. 2007; Zerbi et al. 1978). Two dates of the lava flows suggest Late Pliocene ages (3.9 ± 0.3 and 3.77 ± 0.09 Ma; Fedele et al. 2007; Fibbi 1970).

Tuvonari groups tephrite to phonolite and trachyte lava domes, cryptodomes, flows, and dykes (Figure 3b). Lavas are aphanitic to porphyritic, with a gray to pale blue matrix, with phenocrysts of Sanidine ± Phlogopite ± Plagioclase ± Nepheline ± Hauyne ± Sodalite ± Nosean ± Analcime ± Apatite. Block and ash flow deposits are locally associated with lava domes suggesting that explosive activity accompanied dome emplacement.

Lava from the domes was dated by Beccaluva et al. (1977) and Fedele et al. (2007) with corresponding ages ranging from 3.6 to 3.2 ± 0.2 Ma.

3.2.1.2. Cùglieri subsynthem (Piacenzian). This subsynthem lies in disconformity over older units. It consists of debris avalanche and debris flow deposits associated with major flank collapse of the Ghísos volcano and is grouped in three units:

– Canighèrbu
– Bàdu de Papéri
– Fàche de Sòle

These are respectively associated with three collapse of the north-western and western flanks of the volcanic edifice. The maximum exposed thickness of the deposits is 10 m.

The associated collapse scars are partially exposed. They are horseshoe-shaped, cutting both lava domes and Miocene units (Figures S1, S5, S6 in the map). The debris avalanche deposits present a variability of facies, ranging from breccia containing abundant,

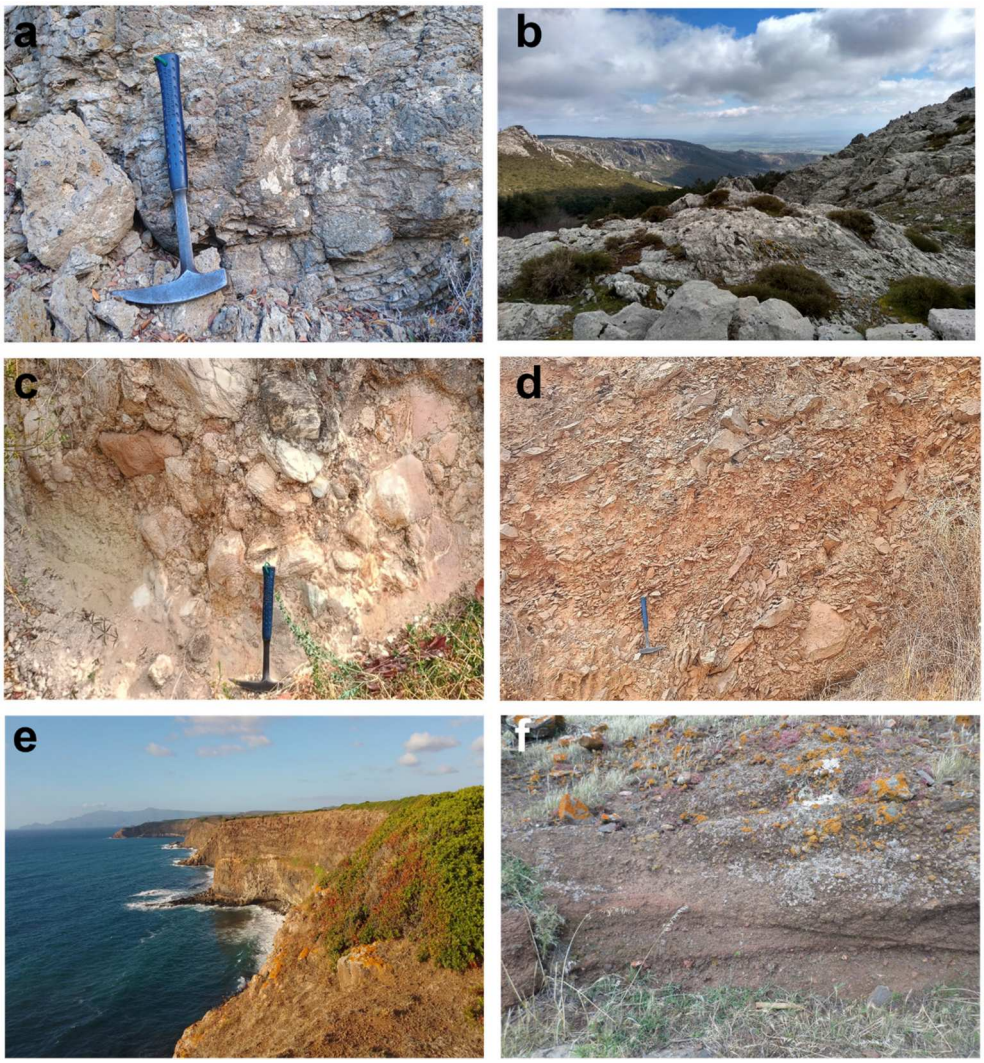

Figure 3. Plio-Pleistocene units of the Montiferru Volcanic Complex. Ghísos Synthem: basanite lava flows of the Pèdra Onàda unit (a); Lava domes of the Sa Tànca Nòa unit (b). Cùglieri Synthem: debris avalanche deposit formed from zeolitized Aúrras Ignimbrites (c); Debris flow deposit containing debris from the Sa Tànca Nòa unit lavas(d). Campèda synthem: trachybasalt aa lava flows and interbedded soils (e). Sèneghe synthem: deposits of the Sa TZepara cinder cone (f).

fractured m-sized clasts (jigsaw-fit), immersed in variable proportions of matrix with varying grain size (Figure 3c, and S5, S6 in the map), to torevas and hummock blocks and more distally, debris flow deposits (Figure S5 in the map). Block and matrix facies are associated with meter-sized blocks and channelization of the flows. All the facies are monomictic and formed after fragmentation of the Sa Tànca Nòa, Santa Caterina, and Aúrras units and the top ignimbrite of the Porto Alabe unit. Mixing among lithologies is observable only at the dm-thick boundaries between different breccia bodies. Hummocks are locally embedded or on top of breccia units. Debris flow deposits are typically composed of platy and angular clasts of Sa Tànca Nòa lava. These deposits can be either massive or stratified, with a variable matrix content (Figure 3d).

The deposits are deeply eroded and partially covered by younger units, are mostly exposed in their proximal portions, and cut by younger volcanic activity of the Campèda synthem.

3.2.1.3. Mùrcuneddu subsynthem. The Mùrcuneddu subsynthem consists of lava domes, clustered in the north-west sector of the Montiferru complex, and tephrite-phonolite and trachyte lava flows. It is in buttress unconformity over the Sa Tànca Nòa subsynthem(Figures S1, S2, S6 in the map) and in disconformity over the Cuglieri subsynthem (Figures S1, S5, S6 in the map). These lavas correspond to the renewed activity of the Ghísos volcano, localized in the Northern area of the Complex (Figures S1 and, S6 in the map). Lavas are compositionally overlapping to the Sa Tànca Nòa ones. Minor pyroclastic deposits (lapilli fallout and PDC) are intercalated with lavas. K/Ar dating of a single lava dome provided an age of 2.8 ± 0.1 Ma Coulon et al. (1974).

3.2.2. Campèda synthem (Piacenzian to Gelasian)

The Campèda synthem groups the lithosomes associated with diffuse volcanic activity (Figure S1 in the map). The synthems lies in angular unconformity

over an erosional surface and paleosols covering the older synthems. It consists of two subsynthems, the Bonarcado and Sèneghe. The subsythems mark a temporal shift in volcanic activity, from diffuse emission of lava flows to monogenetic eruptions.

3.2.2.1. The Bonarcado subsynthem. The Bonarcado subsynthem comprises dark gray to black trachybasalt lava flows and dykes, porphyritic for plagioclase + pyroxene ± olivine, mostly associated with fissure eruptions (Campèda Lavas, Figure 3e) and partially covering the phonolite domes of the Mùrcuneddu unit. Flows are mostly inflated pahoehoe and subordinately 'aa types. They constitute a single lava field, extending for more than 700 km^2. The maximum exposed thickness is along the sea coast and accounts for more than 40 m. Locally, phonolite lava flows cut trachybasalt lava flows. This unit also includes a system of alluvial fans composed by lava and PDC fragments of the Campèda, Ghísos and Sirìsi synthems. The lavas of this synthems are cut by km long transtensional faults, sealed by the deposits and lava flows of the Sèneghe subsynthem.

Various lavas flows were dated by Beccaluva et al. (1973, 1977); Coulon et al. (1974); Fedele et al. (2007) with ages ranging from 3.14 ± 0.08 to 2.5 ± 0.1 Ma.

3.2.2.2. The Sèneghe subsynthem. Sèneghe subsynthem is separated from the Bonarcado subsynthem by an angular unconformity marked by paleosols and localization of volcanic activity.

Sèneghe groups scoria cones (Figure 3f) and lava flows having basanite to trachybasalt composition (Zerbi et al. 1978). Lavas are porphyritic for plagioclase + clinopyroxene + olivine + phlogopite ± apatite crystals and host mantle and crustal xenoliths. Mantle xenoliths are mainly lherzolites, harzburgites, and wehrlites, but websterites and clinopyroxenites are also found in the lavas (Zerbi et al. 1978).

Sèneghe lavas display ages ranging from 2.3 ± 0.2 to 1.57 Ma (Beccaluva et al. 1977; Fedele et al. 2007; Zerbi et al. 1978).

3.2.3. Portovesme synthem

3.2.3.1. Subsynthem of Portoscuso. The synthem, defined in Barca et al. (2005); Pasci et al. (2012) consists of high angle cross-stratified, partially bioturbated sandstones exposed in the northern coastal area of sector (Sechi et al. 2020). The maximum thickness of the exposed deposits is 5 m.

The Portovesme synthem lies in nonconformity over the Sirìsi and Campèda synthems (Figures S1, S2, S5, S6 in the map). The nonconformity is also remarked by the absence of volcanic activity.

3.3. Hydrothermal alteration facies

Hydrothermal altered rocks are exposed in the southern and northern sectors of the studied area, within the Miocene volcanic units. Hydrothermal alteration haloes, associated to quartz-rich ore bodies, are commonly observed in the Sirìsi Synthem breccia and PDC deposits.

Alteration facies were constrained from mineral assemblage reconstructed based on both new XRD analyses and published literature (Table 2).

Within the Miocene caldera, we recognized four alteration facies (Figure S4 in the map), associated

Table 2. Hydrothermal alteration facies.

Alteration facies[1]	Mineral assemblage	Associated ore body	Associated volcanic structure	Epithermal System
Argillic	Microcline, Quartz, Kaolinite, Illite	–	Caldera collapse breccia and subvolcanic intrusions	Miocene Sa Montrarba Low Sulfidation System
Potassic	Orthoclase, Quartz, Albite, Sanidine	Fe-Cu Oxides and Fe-Cu sulfide quartz veins	Caldera collapse breccia	Miocene Sa Montrarba Low Sulfidation System
Hematitization	Hematite, Quartz	Fe-Cu oxides quartz veins	Caldera collapse breccia	Miocene Sa Montrarba Low Sulfidation System
Silicization		Fe-Cu oxides quartz veins and Fe-Cu-Pb-Zn sulfides quartz veins	Caldera collapse breccia	Miocene Sa Montrarba Low Sulfidation System
Propylitic	Quartz, Chlinochlore, Albite, Calcite, Microcline, Biotite, Halloysite	Fe-Cu-Pb-Zn sulfide and oxide veins	Caldera collapse breccia and subvolcanic calc-alkaline bodies.	Miocene Sa Montrarba Low Sulfidation System
Zeolitization	Clinoptilolite-Na, Manganoceladonite, Heulandite, Mordenite	Hot-spring deposits	Tephrite-Phonolite and trachyte Dome complexes	Pliocene–Pleistocene Epithermal Field
Carbonate	Calcite	Hot-spring deposits	Tephrite-Phonolite and trachyte dome complexes	Pliocene–Pleistocene Epithermal Field
Advanced argillic	Quartz, Kaolinite	Hot-spring deposits	Basanite lava vent (cryptodome)	Pliocene–Pleistocene Epithermal Field
Argillic	Magnesiohorneblenda, Montmorillonite, Anortite, Hematite, Fe-tschermakite	Chalcedony-barite veins	Phonolite dome	Pliocene–Pleistocene Cùglieri Epithermal Field
Silicization		Chalcedony-barite veins	Phonolite dome	Pliocene–Pleistocene Epithermal Field

[1]Pirajno (2009).

with Fe-Cu oxide and Fe-Cu-Pb-Zn sulfide quartz rich veins which may have been formed at depths ranging from 360 and 220 m (Fadda 1993). Potassic alteration is the most extended halo and is bordered by a propylitic alteration halo at north, in the caldera rim, and by clay alteration at south. Silicization and hematitization are structurally controlled. Hematitization is associated only to the Fe-Cu oxide veins whereas silicization is associated to both vein types.

In the north sector we recognized five alteration facies (Figure S4 in the map), associated with silica sinter (surficial hot-spring) deposits consisting in chalcedony, agate, microcrystalline quartz, anomalously rich in Au, Ag, As, Hg and chalcedony-baryte (Gold

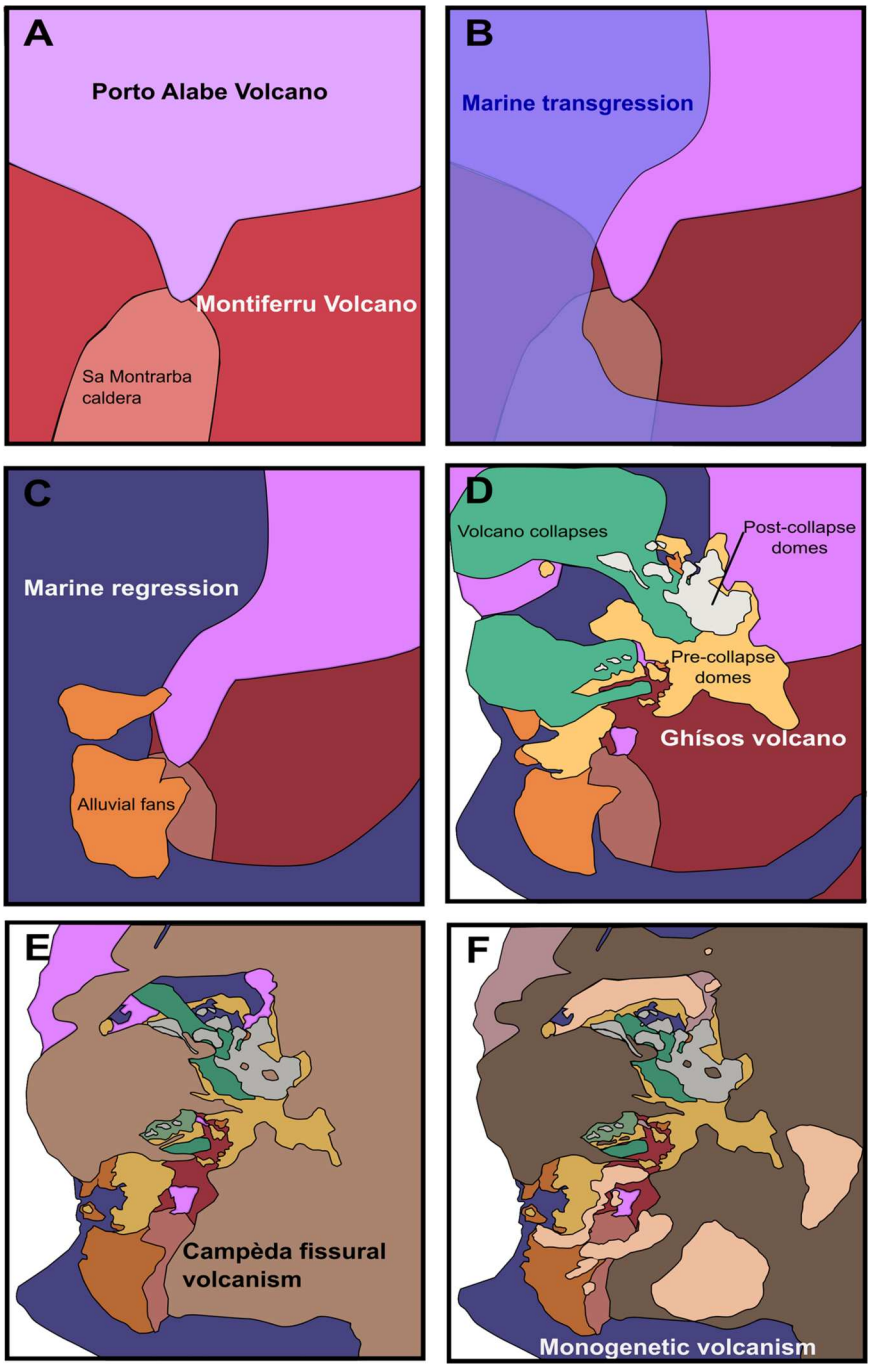

Figure 4. Evolution of volcanic and marine activity in the Montiferru area from Miocene to Late Pleistocene. Early to middle Miocene: A: Formation of the Sirìsi synthem. Two volcanic centers, Sa Montrarba and Porto Alabe, are the cores of Plinian caldera-forming eruptions. The Sa Montrarba volcano is elder than Porto Alabe. B: The volcanic activity is ceased, a marine transgression follows; marls and carbonates sediments deposits in the area (Santa Caterina synthems, Middle to late Miocene). C: Marine regression and continental erosion on Sirìsi Ignimbrites allow the formation of the first Ghísos synthem alluvial fan deposits (Late Miocene –Early Pliocene). D: Lava flows and domes with minor Plinian and volcanic eruptions mark a new volcanic phase (Ghísos). The edifice collapses and the formation of the debris avalanche and debris flow deposits of the Cùglieri synthem (Pliocene). A lava dome field develops at north, partially rebuilding the old edifice. E: Fissural eruptions formed the lava plain of the Campèda (Pliocene–Pleistocene). F: Final monogenetic eruptions of the Campeda (Pleistocene, Sèneghe Synthem).

Mines of Sardinia LTD 2000) and calcite veins. The chalcedony-baryte veins show anomalously high silver concentration, up to 35 ppm (Gold Mines of Sardinia LTD 2000). Fossils leaves, stromatolite bioconstruction and silica eggs are embedded in the chalcedony deposits confirming their formation on surface Hamilton et al. (2019).

4. Discussion

4.1. Geological history of the Montiferru area

4.1.1. Miocene

Stratigraphic observations suggests that two explosive volcanic centers were partially overlapping in the studied area. The southern one, Sa Montrarba, consists of a caldera with welded outflow sheets still exposed outside up to the central portion of the area. Its age is unknown, but stratigraphic observations suggest an Aquitanian age.

The northern one of Burdigalian age, extends beyond the mapped area. In the map it mainly consists of distal facies of large PDC and fallout and minor lava domes (Porto Alabe unit). In the lack of specific data on the source area of the volcanic units, we suppose that they could possibly be buried below the Campèda lava flows N to NE of the studied area.

The Montrarba volcano was already partly eroded by about 18 Ma when the largest eruption of the Porto Alabe unit spread pyroclastic density currents over the entire sector (Figure 4a). The end of volcanic activity was also marked by marine transgression over most of the volcanic complex (Figure 4b).

4.1.2. Plio Pleistocene

The main changes in the tectonic setting lead to uplift of the area and renewal of volcanic activity with emission of primitive magmas from aligned vents in the southern part of the sector (Figure 4c). Further development of crustal magmatic reservoirs led to magma fractionation and contamination (Fedele et al. 2007). Eruption of evolved, volatile poor magma fed effusive activity in the form of lava domes, from vents roughly aligned along SW–NE and W–E structures covering to the center of the studied area, and resulting into a diffuse, 1400 km^3 edifice built over Miocene ignimbrites and limestones and reaching a thickness exceeding 1000 m (Figure 4d). The activity was not significantly affected by partial collapses of the edifices and continued until about 3 Ma.

Stratigraphic data suggest a gradual transition into a new volcanic phase marked by emission of mafic lava flows from fissural sources and construction of the large Campèda lava field which partly covered all the oldest volcanics (Figure 4e). We notice the alternance of phonolite and trachybasalt lava flows in the lower portion of the lava field. This stratigraphy likely suggests the temporary coexistence of magmatic reservoir of magmas with distinct fractionation histories.

Finally, waning of the activity was marked by transtensional tectonics and by the onset of a final eruptive phase of scattered monogenetic eruptions (Figure 4f), whose age is not fully known, but they could at least partly overlap with the monogenetic eruptions occurred in north-west and east (Beccaluva et al. 1983).

4.2. Epithermal phases

Correlation between spatial distribution of the alteration facies, volcanic structures and erosion (Tables 1 and 2) suggests that the hydrothermal alteration may have formed during two distinct stages, respectively Miocene and Pliocene in age. An intracaldera epithermal system formed in the Sa Montrarba volcano, and in a context of calcalkaline magmatism. Both volcanic and hydrothermal activities ended long before the formation of Porto Alabe volcano, whose deposits lie in unconformity over the caldera eroded upper epithermal zone.

An second hydrothermal system developed in the area in Early Pliocene during the alkaline volcanic cycle, possibly associated with dome emplacement and shallow fluid circulation, forming siliceous hot spring deposits. The system developed within the host rocks (Porto Alabe volcano) leading to a second phase of epithermal mineralization of the Miocene volcanics.

5. Conclusions

The 1:50.000 scale volcano-structural map of the Montiferru Volcanic complex provides a comprehensive new review of the geological history of the area. The map highlights the structural framework of the area and two major volcanic phases. An interval of about 14 Ma was characterized by marine transgression. It distinguishes:

Two Miocene volcanic centers marked by explosive volcanism, including a partially exposed and eroded caldera. The activity of the two centers was not coeval but separated by an erosive phase. The second magmatic phase generated:

– Lava dome and flow eruptions of early Pliocene age
– At least three partial collapses of the Ghísos edifice
– A late Pliocene phase of diffuse effusive eruptions building a 1200 km^2 large lava field
– A final Pleistocene phase of scattered, small volume monogenetic eruptions, possibly following about 1 Ma of quiescence.

Two hydrothermal alteration events occurred during the Miocene and Pliocene volcanic cycles, respectively associated with hydrothermal fluid circulation within a caldera and a lava dome field.

Software

The map was produced using the software QGIS (versions 3.4 to 3.34.11-Prizren) and Inkscape (v. 1.4), hereafter referred to simply as QGIS and Inkscape. QGIS was used for digitizing the units, systematizing and storing the data, and creating the maps (main map, alteration map, and union map). Geological cross-sections were initially generated in QGIS 3.34 environment using the qgSurf plugin (release 3.2.2). The final map layout, the schematic representation of units, and the geological cross-sections were completed in Inkscape.

Acknowledgments

We are grateful to A. Funedda for the fruitful discussion on the map, C. Buttau for the help in map layout and design and to S. Andreucci for the essential insights on the most recent sediments exposed in the area.

Disclosure statement

No potential conflict of interest was reported by the author(s).

Funding

We acknowledge the financial support under the National Recovery and Resilience Plan (NRRP), Mission 4, Component 2, Investment 1.1, Call for tender No. 1409 published on 14.9.2022 by the Italian Ministry of University and Research (MUR), funded by the European Union – NextGenerationEU – Project Title WaCoMed – CUP F53D23012390001 – Grant Assignment Decree No. 1388 adopted on 01/09/2023 by the Italian Ministry of Ministry of University and Research (MUR). C Pala was funded by a CNR-IRPI doctoral fellowship (Istituto di Ricerca per la Protezione Idrogeologica, Consiglio Nazionale delle Ricerche and NextGenerationEU).

Data availability statement

The data supporting the findings of this study are available from the corresponding author, upon reasonable request.

References

Allevi, C., Casula, G., Cherchi, A., Chrest, T., & Montadert, L. (2025). The CCenozoic basins of Sardinia (Italy) and their Late Miocene to Present inversion: Insight from new seismic data. *BSGF - Earth Sciences Bulletin*, *196*, 14. https://doi.org/10.1051/bsgf/2025010

Assorgia, A., Beccaluva, L., Deriu, M., Di Battistini, G., Gallo, F., Macciotta, G., Pingani, L., Venturelli, G., Vernia, L., & Zerbi, M. (1981). *Carta Geopetrografica del Complesso Vulcanico del Montiferro (Sardegna Centro-Occidentale)* (I) [Map].

Barca, S., Melis, E., Annino, E., Cincotti, F., Ulzega, A., Orrù, P., & Pintus, C. (2005). *Note Illustrative della Carta Geologica d'Italia alla scala 1:50.000—Foglio 557 Cagliari* (p. 240). APAT Agenzia per la protezione dell'ambiente e per i servizi tecnici, Dipartimeto di difesa del Suolo, Servizio Geologico d'Italia, Regione Autonoma della Sardegna.

Beccaluva, L., Campredon, R., Feraud, G., & Macciotta, G. (1983). Etude des relations entre volcanisme plio-quaternaire et tectonique en Sardaigne à l'aide de l'analyse structurale des dykes. *Bulletin Volcanologique*, *46*(4), 365–379. https://doi.org/10.1007/BF02597771

Beccaluva, L., Campredon, R., Feraud, G., & Macciotta, G. (1983). Etude des relations entre volcanisme plio-quaternaire et tectonique en Sardaigne à l'aide de l'analyse structurale des dykes. *Bulletin Volcanologique*, *46*, 365–379. https://doi.org/10.1007/BF02597771

Beccaluva, L., Deriu, M., Gallo, F., & Vernia, L. (1973). Le vulcaniti post-elveziane del Montiferro occidentale (SSardegna centro-occidentale). *Memorie Della Società Geologica Italiana*, *12*(7), 131–156.

Beccaluva, L., Deriu, M., Macciotta, G., Savelli, C., & Venturelli, G. (1977). Geochronology and magmatic character of the pliocene-pleistocene volcanism in Sardinia (Italy). *Bulletin Volcanologique*, *40*(3), 153–168. https://doi.org/10.1007/BF02596997

Bissig, T., & Cooke, D. R. (2014). Introduction to the special issue devoted to Alkalic porphyry Cu-Au and epithermal Au deposits. *Economic Geology*, *109*(4), 819–825. https://doi.org/10.2113/econgeo.109.4.819

Boi, M., Dessì, R., Fiori, M., Garbarino, C., Grillo, S. M., Humpries, B., Marcello, A., Morris, J., Pilurzu, S., Pretti, S., & Tore, G. (1997). Le potenzialità aurifere della Sardegna. In *Atti giornata di studio "Nuove realtà minerarie in Sardegna"* (pp. 81–113). Ente Minerario Sardo/Associazione Mineraria Sarda.

Carmignani, L., Oggiano, G., Funedda, A., Conti, P., Barca, S., & Pasci, S. (2008). *Carta Geologica della Sardegna Scala 1:250.000* [Map].

Carminati, E., Lustrino, M., & Doglioni, C. (2012). Geodynamic evolution of the central and western Mediterranean: Tectonics vs. Igneous petrology constraints. *Tectonophysics*, *579*, 173–192. https://doi.org/10.1016/j.tecto.2012.01.026

Coulon, C., Demant, A., & Bellon, H. (1974). Premieres datations par la methode K/Ar de quelques laves cenozoiques et quaternaires de sardaigne nord-occidentale. *Tectonophysics*, *22*(1–2), 41–57. https://doi.org/10.1016/0040-1951(74)90034-1

Dannemberg, A. (1905). *Der Vulkanberg Monte Ferru in Sardinien*.

Deriu, M., Rossetti, V., Uras, I., Negretti, C. G., Cau, G., Vardabasso, S., Brotzu, P., & Assorgia, A. (1988). *Capo Mannu—Macomer—Fogli 205-206* (I) [Geological Map]. Regione Autonoma della Sardegna - Servizio dell'Attività Mineraria.

Di Battistini, G., Montanini, A., & Zerbi, M. (1990). *Geochemistry of volcanic rocks from southeastern Montiferro. Neues Jahrbuch für Mineralogie. Abhandlungen*, *162*, 35–67.

Faccenna, C., Speranza, F., Caracciolo, F. D., Mattei, M., & Oggiano, G. (2002). Extensional tectonics on Sardinia (Italy): Insights into the arc–back-arc transitional regime. *Tectonophysics*, *356*(4), 213–232. https://doi.org/10.1016/S0040-1951(02)00287-1

Fadda, R. (1993). *Prospezione del sistema epitermale del settore sud-occidentale del Montiferru (Sardegna Centro-Occidentale). Le alterazioni e le mineralizzazioni metallifere* [PhD dissertation]. Università degli Studi di Cagliari.

Fadda, S., Fiori, M., & Pretti, S. (1998). The sandstone-hosted Pb occurrence of Rio Pischinappiu (Sardinia, Italy): A Pb-carbonate end-member. *Ore Geology Reviews*, *12*(5), 355–377. https://doi.org/10.1016/S0169-1368(98)00008-0

Fedele, L., Lustrino, M., Melluso, L., Morra, V., & d'Amelio, F. (2007). The Pliocene Montiferro volcanic complex (central-western Sardinia, Italy): Geochemical observations and petrological implications. *Periodico Di Mineralogia*, *76*, 101–136. https://doi.org/10.2451/2007PM0011

Fibbi, A. (1970). *Il vulcanismo terziario basico della SSardegna Nord-Occidentale*. Università degli Studi di Pisa.

Gold Mines of Sardinia LTD. (2000). Annual Report 31 Decemeber 2000, s.l.

Grillo, S. M., Sistu, G., Fadda, R., & Fiori, M. (1993). Le alterazioni potassiche epitermali del Montiferru (Sardegna centro-occidentale). *Bollettino della Società Geologica Italiana*, *112*, 647–657.

Hamilton, A. R., Campbell, K. A., & Guido, D. M. (2019). *Atlas of siliceous hot spring deposits (sinter) and other silicified surface manifestations in epithermal environments* (GNS Science report; 2019/06). GNS Science.

Kelley, K. D., & Spry, P. G. (2016). Critical elements in alkaline igneous rock-related epithermal gold deposits. In P. L. Verplanck, & M. W. Hitzman (Eds.), *Rare earth and critical elements in ore deposits* (pp. 195–216). Society of Economic Geologists. https://doi.org/10.5382/Rev.18.09

Kelley, K. D., Spry, P. G., McLemore, V. T., Fey, D. L., & Anderson, E. D. (2020). *Alkalic-Type Epithermal Gold Deposit Model: Chapter R in Mineral Deposit Models for Resource Assessment* (Scientific Investigations Report) [Scientific Investigations Report].

La Marmora, A. F. (1857). Troisième partie. Description géologique. In *Voyage en sardaigne, ou description statistique, physique et politique de cette ile, avec des recherches sur ses productions naturelles et ses antiquités* (pp. 1–730). Fratelli Brocca, Veuve Arthus Bertrand.

Mancosu, A., Nebelsick, J. H., & Buosi, C. (2022). Drilling predation on spatangoid echinoids from the Miocene of Sardinia: A taphonomic and paleoecological perspective. *Journal of Paleontology*, *96*(5), 1132–1148. https://doi.org/10.1017/jpa.2022.28

Miall, A. D. (2006). *The geology of fluvial deposits*. Springer Berlin Heidelberg. https://doi.org/10.1007/978-3-662-03237-4

Ministero dell'Industria e Commercio. (1940). *Relazione sul servizio minerario e statistica delle industrie estrattive in italia nell'anno 1940*. Istituto Poligrafico dello Stato, Roma.

Montanini, A., & Harlov, D. (2006). Petrology and mineralogy of granulite-facies mafic xenoliths (Sardinia, Italy): Evidence for KCl metasomatism in the lower crust. *Lithos*, *92*(3–4), 588–608. https://doi.org/10.1016/j.lithos.2006.03.053

Moscati, S., Bartoloni, P., & Bondì, S. F. (1997). *La penetrazione fenicia e punica in Sardegna. Trent'anni dopo*. Vol. IX (I). MemANL.

Pasci, S., Carmignani, L., Pisanu, G., Sale, V., Ulzega, A., Orrù, P., Pintus, C., & Deiana, G. (2012). *Note Illustrative della Carta Geologica d'Italia alla scala 1:50.000—Foglio 554 Carbonia* (p. 271). APAT Agenzia per la protezione dell'ambiente e per i servizi tecnici, Dipartimeto di difesa del Suolo, Servizio Geologico d'Italia, Regione Autonoma della Sardegna. https://www.isprambiente.gov.it/Media/carg/note_illustrative/564_Carbonia.pdf

Pirajno, F. (2009). *Hydrothermal processes and mineral systems*. Springer Netherlands. https://doi.org/10.1007/978-1-4020-8613-7

Salvador, A. (1987). Unconformity-bounded stratigraphic units. *Geological Society of America Bulletin*, *98*(2), 232. https://doi.org/10.1130/0016-7606(1987)98<232:USU>2.0.CO;2

Savelli, C., Beccaluva, L., Deriu, M., Macciotta, G., & Maccioni, L. (1979). K/Ar geochronology and evolution of the tertiary "calc-alkalic" volcanism of sardinia (Italy). *Journal of Volcanology and Geothermal Research*, *5*(3–4), 257–269. https://doi.org/10.1016/0377-0273(79)90019-2

Sechi, D., Andreucci, S., Stevens, T., & Pascucci, V. (2020). Age and significance of late Pleistocene Lithophyllum byssoides intertidal algal ridge, NW Sardinia, Italy. *Sedimentary Geology*, *400*, 105618. https://doi.org/10.1016/j.sedgeo.2020.105618

Simmons, S. F., White, N. C., & John, D. A. (2005). Geological characteristics of epithermal precious and base metal deposits. In J. W. Hedenquist, J. F. H. Thompson, R. J. Goldfarb, and J. P. Richards (Eds.), *One hundredth anniversary volume*. Society of Economic Geologists.

Zerbi, M., Giammetti, F., Gallo, F., & Vernia, L. (1978). Mineralogia dei noduli peridotitici delle basaniti analcitiche superiori del Montiferru, Sardegna. *Ateneo Parmense, Acta Naturalia*, *14*, 421–463.